Journal of Building Engineering 108 (2025) 112867

Contents lists available at ScienceDirect

Journal of Building Engineering

journal homepage: www.elsevier.com/locate/jobe

Sustainable earthen plasters: surface resistance enhancement via thermal treatments

Marta Cappai [a,b,*], Giorgio Pia [a,b]

[a] Dipartimento di Ingegneria Meccanica, Chimica e dei Materiali, Università degli Studi di Cagliari, Piazza d'Armi, 09123, Cagliari, Italy
[b] Materialia Association, San Gavino Monreale, 09037, Sardinia, Italy

ARTICLE INFO

Keywords:
Clay-based plaster
Stabilization
Heat-treatment
Erosion resistance
Water resistance

ABSTRACT

The construction sector contributes approximately 37 % of global embodied carbon from materials. Earth-based materials offer a more sustainable alternative, and using recycled aggregates as sand substitutes further reduces environmental impact by limiting raw material extraction. However, these materials are often vulnerable to erosion and water action. This study investigates low-temperature thermal treatments (200–600 °C) of 10 and 60 min and bio-based polymer coatings to enhance the durability of clay-based mixtures with recycled aggregates. Treatments at 500–600 °C significantly improved resistance, with short treatments at 600 °C performing comparably to longer ones. In contrast, bio-based coatings were less effective due to superficial application and film discontinuities. Results highlight the potential of in situ thermal stabilization as a sustainable and efficient method to improve the durability of earthen construction materials and promote their use as a viable alternative in sustainable building practices.

1. Introduction

The construction and building materials sector is among the most significant in terms of energy consumption and, therefore, environmental impact. To date, most efforts have focused on the *operational carbon* which pertains to emissions resulting from the heating, cooling, and lighting of buildings, as well as the energy consumption of internal devices [1–7]. In this respect, relevant progress has been made, with the aim of reducing the sector's contribution from 75 % to 50 % over the coming decades [8]. However, substantial progress can only be achieved by simultaneously addressing the *embodied carbon* which relates to the production processes of construction materials such as cement, metals, and ceramics used in buildings. This significant portion of the market is classified as highly energy-intensive, and it is estimated to be responsible for 37 % of global emissions [9].

The reasons why this sector has received less attention in terms of reducing its environmental and energy impact are linked to several factors, including: (a) the complexity of the production chain, which involves multiple stakeholders with different roles and functions (e.g., complex supply chains for raw materials, fragmentation of preliminary production phases, and long life cycles of infrastructure and technologies); (b) insufficient awareness and the slow adoption of life cycle assessment (LCA) tools and methodologies; and (c) the economic costs associated with process improvements [9,10].

These factors have made it difficult to develop effective strategies capable of attracting political and financial attention towards a transition path. Nonetheless, there is now widespread recognition of the urgent need to take action to achieve rapid decarbonization in

* Corresponding author. Dipartimento di Ingegneria Meccanica, Chimica e dei Materiali, Università degli Studi di Cagliari, Piazza d'Armi, 09123 Cagliari, Italy.
E-mail address: marta.cappai@unica.it (M. Cappai).

https://doi.org/10.1016/j.jobe.2025.112867
Received 19 January 2025; Received in revised form 18 April 2025; Accepted 5 May 2025
Available online 6 May 2025

this sector. The primary goal is to reach net-zero emissions by 2050 [11,12]. This result can only be achieved by improving production process efficiency, increasing the use of bio-based materials, and expanding reuse and recycling policies. In this context, the use of earth as a sustainable building material has gained increasing importance, particularly for the construction of smaller-scale buildings [13,14]. Earth is widely available and can be processed locally by mixing it with water and fibrous materials of natural origin [15–18]. The resulting artifacts, following these principles, can be highly reusable and recyclable. Additionally, their significant mass contributes positively to indoor comfort, especially in arid climates, where extreme day-night temperature fluctuations can be significantly mitigated [19–22].

Currently, only 8–10 % of the global population lives in earth-constructed buildings (compared to 33 % at the end of the 20th century), with the majority concentrated in less economically developed countries such as Bangladesh, the Democratic Republic of Congo, Nigeria, and Ethiopia [23]. In these contexts, earth-based materials have often been used without proper attention to technical guidelines, increasing the perception of inefficiency. However, growing environmental awareness is leading to a resurgence of interest in using earth-based materials in high-end applications that aim to adapt traditional construction practices to contemporary standards [15,16,18,24–35]. Addressing the weaknesses of clay-sand-water-fiber materials, which are inherently susceptible to water damage and surface wear, is crucial [36–40]. Recent literature is rich in studies focusing on the stabilization of earthen material. Some methods derive directly from traditional practices using natural polymers, while others incorporate historical and modern binders (lime and cement), bio or synthetic polymers as additives, and still others apply thermal treatments [18,24,27,41–60].

For example, Kariyawasam and Jayasinghe [61] present a detailed study on the stabilization of compressed earth materials for construction (cement-stabilized rammed earth). The authors utilized three types of soils and identified sandy laterite as the most suitable base material. Mechanical tests showed satisfactory results for samples with cement contents exceeding 6 %, with flexural strength comparable to that of fired clay bricks. However, some challenges were observed in field durability tests, particularly with respect to capillary water absorption and surface erosion rates [61].

Bruno et al. [62] propose a study on the stabilization of earth-based materials using hydrated lime and guar gum for sustainable construction. The results indicated that the mechanical properties of the stabilized materials exceeded those of untreated systems, with increased load-bearing capacity and stiffness inversely proportional to the guar gum content. Thermal properties showed no significant differences, with values similar to those of untreated systems. The biopolymer-treated samples did not show improvements in hygroscopic behaviour, while the hydrated lime-treated ones exhibited greater moisture resistance [62].

Real et al. [63] used recycled cement from demolition waste as a stabilizer for earthen artifacts. The experimental results demonstrated significant performance improvements. After stabilization, water absorption decreased by up to 25 % in systems using clayey soil, while an increase of 22 % was observed in systems made with sandy soil. The use of recycled cement resulted in greater water absorption compared to systems stabilized with Portland cement, which was attributed to the reduced pore size and, consequently, finer porosity [63].

Atzeni et al. [51] studied the surface resistance of earthen materials by comparing untreated systems with those stabilized using various polymers, lime, and Portland cement, as well as thermally treated specimens subjected to sandblasting tests. The results did not show a clear correlation between microstructural data and the weight loss induced by particle impact. The highest surface resistance was observed in the samples treated with organic polymers. Lime and cement binders did not lead to significant improvements in mechanical or wear resistance but positively affected dimensional stability during curing. Thermal treatments improved mechanical strength, water resistance, and surface hardness [51].

Godoy et al. [50] conducted a study on earthen plasters stabilized through short surface heat treatments at 400 °C. The results showed improvements in mechanical properties and surface wear resistance, while a decrease in shear strength and adhesion was observed [50].

In general, different stabilization techniques exhibit both strengths and weaknesses. While thermal treatment entails energy consumption, chemical treatment may pose challenges in terms of compatibility with reuse and recycling, especially when synthetic organic components are significant. Despite the growing number of studies on the stabilization of earth-based materials, few works focus on low-temperature thermal treatments, reduced exposure times, and aging techniques under controlled conditions [24,47–51,64,65]. In particular, in the specific case of erosion caused by particle impact on surfaces, there is a lack of methods in which the experimental setup involves a limited number of variables to control [40,51,66–70].

This work presents a systematic study aimed at enhancing water and surface erosion resistance through low-temperature thermal treatments with different exposure times. The materials analyzed are clay-based and incorporate recycled aggregates sourced from previous demolitions. The obtained results have been compared with equivalent systems that were either untreated or surface-treated with bio-based polymers. Furthermore, a new experimental technique based on the use of the Spex Miller is introduced for erosion testing.

The results obtained are intended to propose highly sustainable and recyclable materials as primary components for construction (either in small-scale structures or in limited elements of larger buildings), in place of energy-intensive binders such as lime and cement, thereby promoting on-site recycling and reducing embodied emissions and transportation costs.

2. Materials and methods

The raw materials used to prepare the different mix designs were clay and recycled aggregates from demolition waste. The clay came from a quarry in Lozzolo, Vercelli (Italy). The demolition waste, supplied by R.E.R. Srl (Is Seddas – Quartucciu – Sardinia, Italy), was macroscopically heterogeneous, with visible fragments of stone, soil, earthen and lime mortars, plastic, and wood. The latter two fractions (plastic and wood) were removed through a pre-washing process. Specifically, to obtain the recycled aggregates, the

demolition waste was immersed in distilled water and mixed. After 12 h, floating plastic and wood fragments were removed from the surface. This procedure was repeated several times until no plastics or wood were observed on the water surface. The aggregate was then dried for 24 h at 100 °C in an oven, and subsequently sieved to ensure a maximum particle size below 2 mm. Clay and recycled aggregates were characterized by X-ray diffraction (XRD) using a Bruker D8 Advance diffractometer equipped with a multi-mode LYNXEYE XE-T detector and Cu Kα radiation. Particle size distribution was determined by laser light scattering analysis using a CILAS 1180 instrument.

Two bio-based polymers, namely S and D, were selected and applied as protective coatings to evaluate their effectiveness in improving water and erosion resistance of the particles, and to compare their performance with that of thermal treatments. S is a short oil alkyd emulsion, while D is a urethane–alkyd dispersion. The main characteristics of S and D are reported in Table 1 [71–74].

Clay and recycled aggregates were mixed in different proportions with distilled water. The weight ratios of the prepared mixtures are shown in Table 2.

For the preparation of the samples, clay and recycled aggregates were combined in the dry state according to the proportions reported in Table 2 and manually mixed for 60 s in a container to ensure homogenization. Distilled water was then gradually added and the mixture was mixed using an electric mixer for 5 min. After the mechanical mixing process, the mixture was allowed to rest for 5 min to promote more effective hydration of the components. Finally, a further brief mechanical mixing was performed for 30 s, after which the mixture was inserted into molds with the aid of a spatula to obtain the samples.

The samples were manufactured using circular metal molds with an internal diameter of 45 mm and a thickness of 6 mm. These were dried for 48 h under laboratory conditions and then placed in a desiccator for 30 days before use. Dimensional shrinkage was measured using a calliper by evaluating the change in diameter and thickness.

The different mixtures were then subjected to erosion tests. The series of samples that showed the least weight loss and, consequently, the highest resistance to erosion were then treated with the various stabilization methods. For each series, 10 samples were tested, and the result is the average value expressed in kg/m^2.

Erosion was simulated using a SPEX Mixer/Mill 8000, a high-energy mill widely used in mechanochemistry for the grinding of powders contained within a stainless-steel vial [75]. This vial consists of a cylindrical container with an outer diameter of 2.4 cm, an inner diameter of approximately 1.9 cm, and an internal height of approximately 5.8 cm. It provides the chamber in which the powders and grinding balls are placed for processing. The vial is sealed with a stainless-steel cap and a threaded aluminum cap. In this study, the erodent material was placed inside the vial, while the steel cap was replaced with the sample to be eroded. A quartz sand, with nominal average diameter of 300 μm was used as erosive agent [40,68,76]. Selected sand was added to the vial as an erodent agent in the amount of 0.2 g. The samples were positioned in place of the vial cap. In particular, prior to testing, the samples were reinforced along the edges with a layer of two-component epoxy resin to minimize wear due to their placement in the Spex jar. A seal made of PVC with a thickness of 0.1 mm was inserted between the vial and the sample. Once the test began, the SPEX Mixer/Mill 8000 induced a complex motion in the vial, characterized by a three-dimensional trajectory combining a vertical harmonic component and partial rotation [75]. This motion causes the erodent material inside the vial to repeatedly impact the surface of the sample. Each sample was subjected to cycles of 5 min, and the weight loss was measured at the end of each cycle. A total of 12 cycles were performed for each sample. At the end of the erosion tests, the mixture with the highest erosion resistance was identified and its stabilization was studied.

The selected mixture was then subjected to different thermal treatments to study the effects of surface stabilization. The temperatures studied were 200 °C, 300 °C, 400 °C, 500 °C, and 600 °C. For each temperature, two treatment times were investigated: 10 min (samples named A) and 60 min (samples named B). For each treatment, 10 samples were prepared for the erosion test, 10 for water absorption, and 10 for wet-dry cycles. The same thermal treatments were also performed on the raw materials (clay and recycled aggregates), and the powders were subsequently analyzed by XRD to detect mineralogical changes.

Additionally, two more series of samples were prepared, which involved the use of bio-based polymers. These were diluted to 20 % w/w with distilled water, mixed thoroughly, and applied evenly to the sample surfaces with a brush. The samples were then left to dry under laboratory conditions for one week before undergoing erosion, water absorption, and wet-dry cycle tests. The series made with the bio-based polymers are named with either S or D at the end of the name, depending on the polymer used. Also in this case, 10 samples were prepared for each test in every series.

Erosion tests were performed for each sample series (those thermally treated and those stabilized with bio-based polymer) as described earlier.

Total sample absorption was evaluated through complete imbibition, with samples weighed at regular intervals (every minute for the first 10 min, and then every 5 min thereafter, for a total test duration of 360 min). For samples that retained their shape during imbibition and exhibited no loss of cohesion between grains, the mass of water absorbed was evaluated relative to the mass of the dried sample. This evaluation enabled the assessment of the volume of water-accessible pores over the defined total absorption period.

Wet-dry cycles were conducted by immersing the samples in distilled water at room temperature (20 °C ± 2 °C) for 20 min, followed by heating in an oven (160 °C ± 2 °C) for 40 min. At the end of each immersion and drying phase, the weight of each sample was measured. A total of 40 cycles were performed on the samples that successfully completed the test.

Table 1
Short oil alkyd emulsion (S) and urethane–alkyd dispersion (D) characteristics.

	State	Appearance	pH	Bio-based content (%)	Density (g/cm^3)	Dynamic viscosity (at 20–25 °C)
S	Liquid	Slightly yellowish	7.0–9.0	>95	1.02–1.03	<1000 mPa s
D	Liquid	White, milky	6.0–8.0	>43	1.05	10 ÷ 500 mPa s

Table 2
Mixtures made with clay and recycled aggregates. The indicated proportions refer to the weight of the different components in the mixture.

Mixture type	Clay	Recycled Aggregate	Water
M1	4	4	2
M2	3	5	2
M3	2	6	2

A flowchart illustrating the different experimental steps involved in the study is shown in Fig. 1.

3. Results and discussion

3.1. Raw materials and mix design characterization

XRD analyses have shown that the clay is composed of quartz, albite, illite, interstratified illite/montmorillonite, interstratified illite/chlorite, and traces of kaolinite. The mineralogical principal phases identified in recycled aggregates include quartz, calcite, feldspar, muscovite/illite and kaolinite.

Granulometric analysis has been conducted on clay and recycled aggregates and the resulting particle size distribution curves are shown in Fig. 2. The clay exhibits a predominantly fine-grained distribution, with approximately 94 % of particles smaller than 0.1 mm. In contrast, the recycled aggregate presents a significantly coarser and broader distribution, with most particles ranging from approximately 0.1 mm–2 mm. This indicates its function as a structural component, contributing to the dimensional stability of the mixtures.

The raw materials were mixed with distilled water according to the proportions given in Table 2, and samples of M1, M2, and M3 were prepared. After the drying process, the samples exhibited different levels of shrinkage, which decreased with increasing recycled aggregates content in the mixture. Specifically, the M1 samples showed the highest shrinkage, with a diameter reduction of 1.75 mm; the M2 samples exhibited intermediate shrinkage, with a reduction of 1.55 mm, whereas the M3 samples displayed the smallest diameter reduction, measuring 1.00 mm. The height of 6 mm, however, remained unchanged across all sample types.

Visually, the M1 samples exhibit greater chromatic uniformity, with the fine grain remaining on the surface after application, resulting in smooth and colour-consistent surfaces (Fig. 3 a). Conversely, the M3 samples display high surface roughness and less chromatic uniformity due to the prominent recycled aggregates grains visible on the surface (Fig. 3 c). The M2 samples represent intermediate conditions (Fig. 3 b).

3.2. Erosion resistance of M1, M2 and M2 samples

Erosion tests conducted on the samples revealed a clear relationship between material composition and erosion resistance. Samples prepared with varying proportions of clay, recycled aggregates, and water exhibited distinct behaviours under particle impact.

In Fig. 4, the angular coefficients of the best correlation lines between the experimental points obtained from the erosion cycles

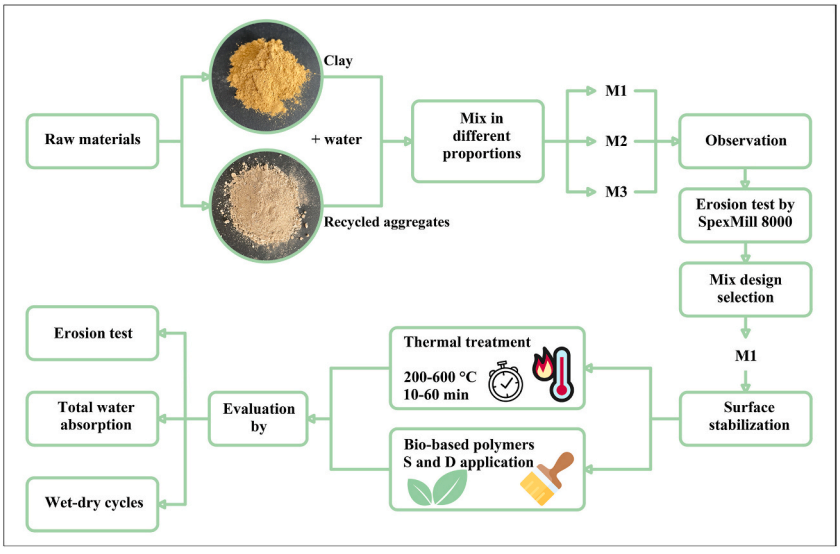

Fig. 1. Flowchart of the different experimental steps.

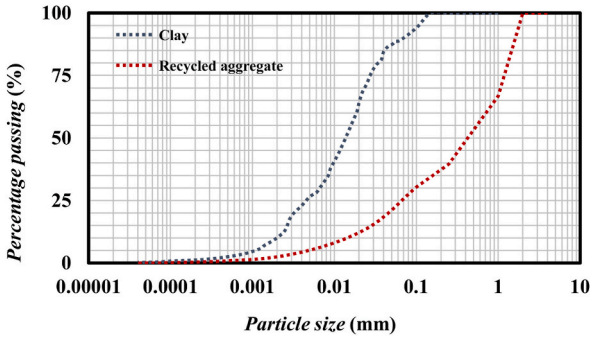

Fig. 2. Particle size distribution of clay and recycled aggregates.

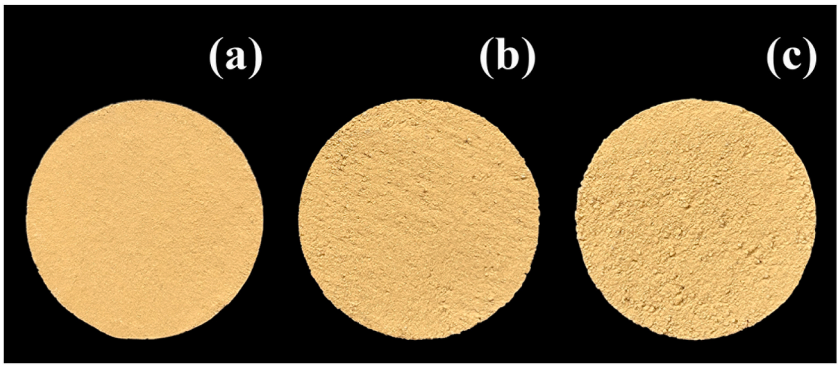

Fig. 3. Surfaces of samples M1 (a), M2 (b), and M3 (c).

represent the speed of the degradation process of individual systems (erosion rate: ER). The greater the absolute value, the higher the ER (Table 3). Thus, these values can be used as a basis for comparison to describe the phenomenon.

Samples with a higher clay content, such as M1, proved to be more resistant to erosion than those with a higher recycled aggregates content, such as M3 (Fig. 4). This behaviour is attributable to the plastic nature of clay, which absorbs impact energy through permanent deformation rather than breaking. The smooth and homogenous surface of the samples M1, achieved through the clay's ability to create a compact matrix, also reduces the exposure of recycled aggregates grains and limits the impact points of erosive particles. In the series with a higher recycled aggregates content, erosion is primarily attributed to the disintegration of the matrix, which compromises the system's cohesion, despite the higher intrinsic hardness of the exposed mineralogical species. This is consistent with the findings of other authors on similar materials subjected to different erosion tests [51].

Samples with a higher recycled aggregates content exhibit a more irregular surface, where exposed grains serve as weak points (Fig. 5). Under impact, micro-cracks form at the points of contact with the matrix. The inherent brittleness of recycled aggregates promotes grain fragmentation and detachment, leading to an increased loss of material. The type of erosion observed is attributable to localized particle impacts, with compressive, shear and tensile stresses acting simultaneously. In samples with more clay, a plastic

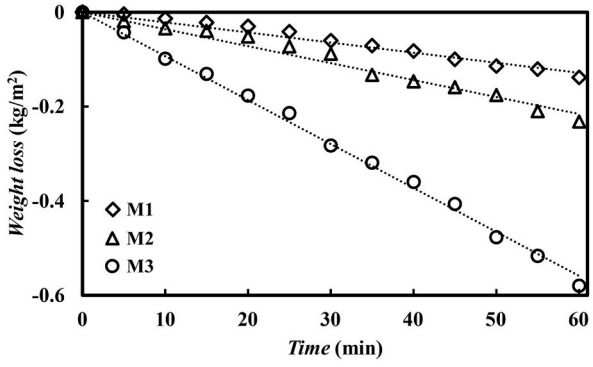

Fig. 4. Weight loss measured on samples M1 (◊), M2 (△), and M3 (○) during erosion cycles.

Table 3
ER (kg/m^2·min) for the different mixture.

Sample series	ER ($-1{\cdot}10^{-3}$ kg/m^2·min)
M1	2.1
M2	3.6
M3	9.3

response prevails, while brittle fracturing predominates in samples with more recycled aggregates. These findings are consistent with previous studies, particularly with Atzeni et al. [51], where similar earth-based systems showed that increasing sand content in the mixture leads to higher surface erosion due to reduced interparticle cohesion.

These results confirm that increasing the clay fraction improves erosion resistance, both due to the inherent mechanical properties of the material and the protective effect of the smooth and uniform surface.

3.3. M1 samples subjected to thermal and bio-based polymer treatments

The results obtained from erosion tests conducted on the different mixtures guided the selection of the sample composition for studying the effects of surface treatment. Considering the higher erosion resistance of the M1 samples, this mixture was chosen for the study of surface stabilization treatments. To perform different treatments, samples from the M1 series have been divided into two groups: group A, treated for 10 min; and group B, treated for 60 min. The new acronyms have been designed to explicitly include the treatment temperature (consequently, a sample originally belonging to the M1 series and treated for 10 min at 600 °C has been henceforth referred to as A600).

Fig. 6 was developed to qualitatively illustrate the colour variations resulting from thermal treatments. All treated sample series exhibited evident qualitative changes in both colour (Fig. 6) and weight (Table 4). Heat-treated samples displayed a colour shift from brown to orange, with the change occurring more rapidly in the series treated for 60 min (Fig. 6f–j). This observation suggests that treatment duration significantly influences the properties of the systems. Samples treated with bio-based polymers demonstrated slight colour saturation and the development of a mildly glossy surface (Fig. 6k and l).

The thermally treated series showed a weight reduction, with treatments extending to 60 min resulting in a more pronounced weight decrease compared to samples treated for only 10 min (Table 4). In contrast, the application of bio-based polymers led to an average weight increase of approximately 1.54 % ± 0.5 for the samples treated with polymer S and 1.57 % ± 0.6 for those treated with polymer D (Table 4).

The mineralogical variations induced by heat treatment have been studied on the powdered raw materials using X-ray diffraction (XRD). Given the temperatures used in the experiment and the mineralogical composition of the raw materials, the most significant transformations have been observed in the clay minerals present in the samples.

In the case of clay, increasing temperature has led to a progressive reduction in the intensity of low-angle peaks associated with mixed phases such as illite/montmorillonite and interstratified illite/chlorite. Fig. 7a shows the XRD patterns of the untreated sample and those thermally treated at 300 °C and 600 °C. A comparison of Fig. 7a and b highlights that the intensity of the peaks at 300 °C for samples treated for 10 min has been higher than that observed for powders thermally treated for 60 min. This indicates that heat treatment time has significantly influenced the extent of mineralogical transformations, particularly dehydration process, which have been highly time-dependent at these temperatures. At 600 °C, the intensity of the low-angle peak has almost completely disappeared, while the peaks associated with kaolinite have been entirely eliminated due to the collapse of the kaolinite lattice, which occurs at approximately 500 °C [77,78]. This behaviour is consistent in samples subjected to heat treatment for both 10 and 60 min. This suggests that at temperatures between 500 °C and 600 °C, even short heat treatment durations (10 min) have been sufficient to induce substantial structural changes in the lattices of clay minerals.

In contrast, the XRD patterns of recycled aggregates (Fig. 7c and d) have shown only the disappearance of kaolinite peaks, as this

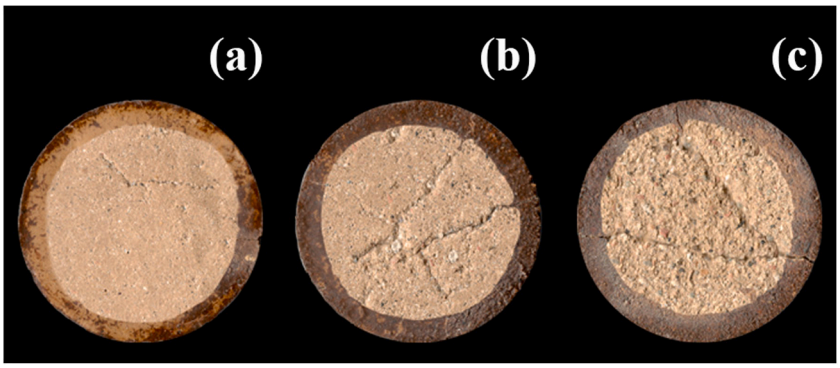

Fig. 5. Samples M1 (a), M2 (b), and M3 (c) after completing the erosion cycles.

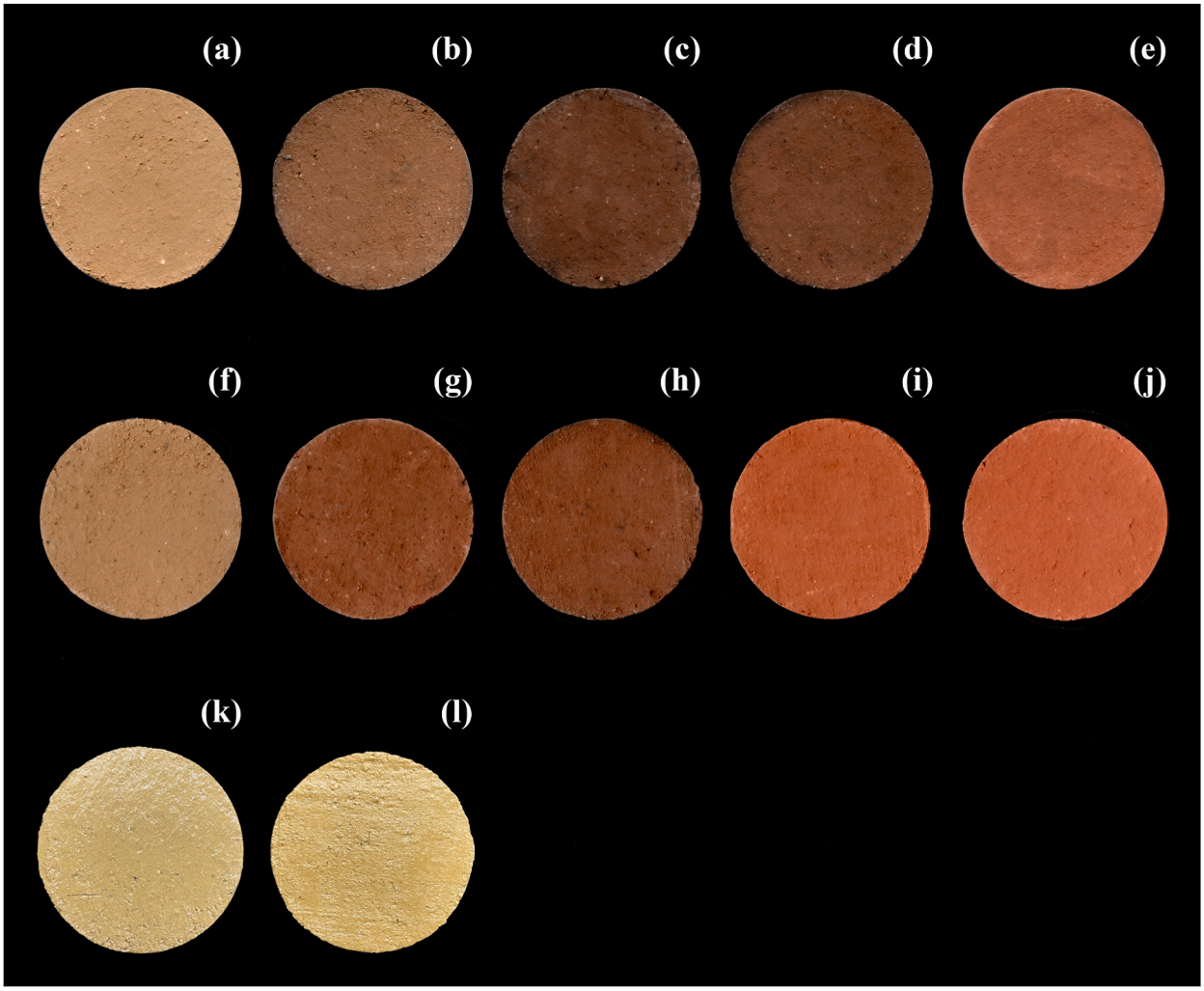

Fig. 6. Surfaces of the samples subjected to superficial stabilization: A200 (a); A300 (b); A400 (c); A500 (d); A600 (e); B200 (f); B300 (g); B400 (h); B500 (i); B600 (j); M1_S (k); M1_D (l).

Table 4
Weight variations of M1 samples subjected to surface treatments.

Samples	Temperature (°C)	Treatment time (min)	Weight variation after treatment (%)
A200	200	10	0.66 ± 0.05
A300	300	10	1.73 ± 0.09
A400	400	10	2.74 ± 0.1
A500	500	10	3.5 ± 0.06
A600	600	10	4.62 ± 0.11
B200	200	60	0.86 ± 0.05
B300	300	60	2.14 ± 0.09
B400	400	60	3.87 ± 0.1
B500	500	60	4.9 ± 0.06
B600	600	60	5.68 ± 0.11
M1_S	–	–	1.54 ± 0.5
M1_D	–	–	1.57 ± 0.6

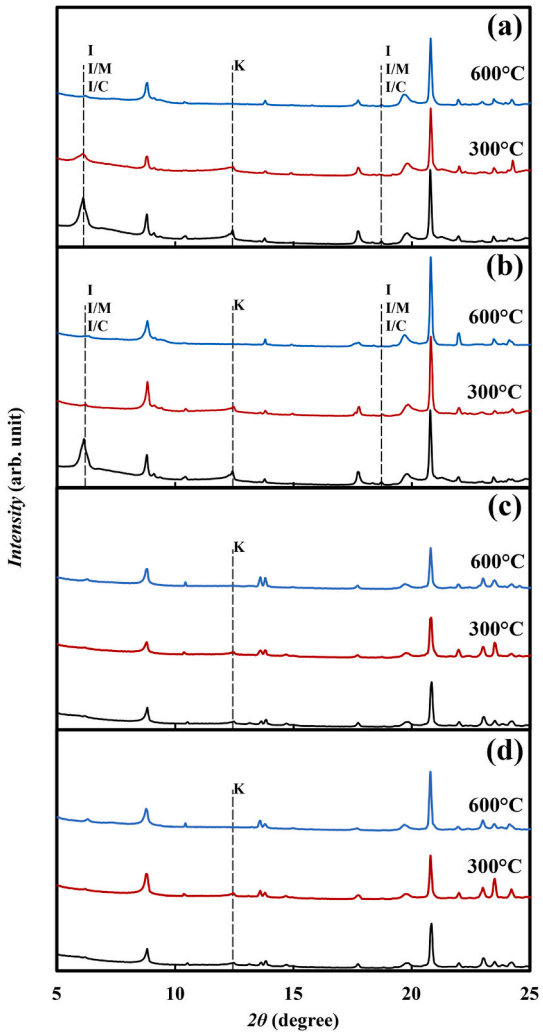

Fig. 7. XRD patterns of clay and recycled aggregates powders subjected to heat treatment. Clay thermally treated for 10 min (a) and 60 min (b). Recycled aggregates thermally treated for 10 min (c) and 60 min (d). Untreated sample (black); sample treated at 300 °C (red); sample treated at 600 °C (blue).

material does not contain swelling clay minerals, unlike clay.

3.4. Erosion resistance of M1 treated samples

The results obtained on the surface-treated samples subjected to erosion tests are shown in Fig. 8.

Samples subjected to heat treatment for only 10 min (Fig. 8 a) exhibit a progressive weight loss as the temperature increases. In particular, those treated at 200 °C showed behaviour very similar to that of untreated samples. This effect can be attributed to the fact that, at 200 °C and for such a short duration, structural changes in the material matrix are limited. The clay matrix, therefore, retains the cohesion and plasticity typical of untreated material, the extent of the treatment is insufficient to induce a significant change, and the sample behaves as if it had not been treated.

The increase in the ER (Fig. 9, in blue) with rising temperature is moderate and occurs up to 400 °C. At 500 °C, however, a trend reversal is observed, with an increase in erosion resistance compared to samples treated at lower temperatures. Nevertheless, samples treated at 500 °C do not show any improvement compared to untreated ones. A marked decrease in erosion susceptibility is observed only for samples subjected to heat treatment at 600 °C (A600), where the XRD patterns no longer show the peaks associated with mixed illite/montmorillonite, illite/interstratified chlorite, and kaolinite layers (Fig. 7).

Samples subjected to heat treatment for 60 min (Fig. 8 b) show a more pronounced weight loss after erosion, leading to a higher ER compared to those treated for only 10 min (Fig. 9, in red). This increased weight loss is particularly evident up to a temperature of 400 °C. However, at treatment temperatures of 500 °C and 600 °C, the erosion susceptibility of the samples decreases significantly, becoming even lower than that of untreated samples.

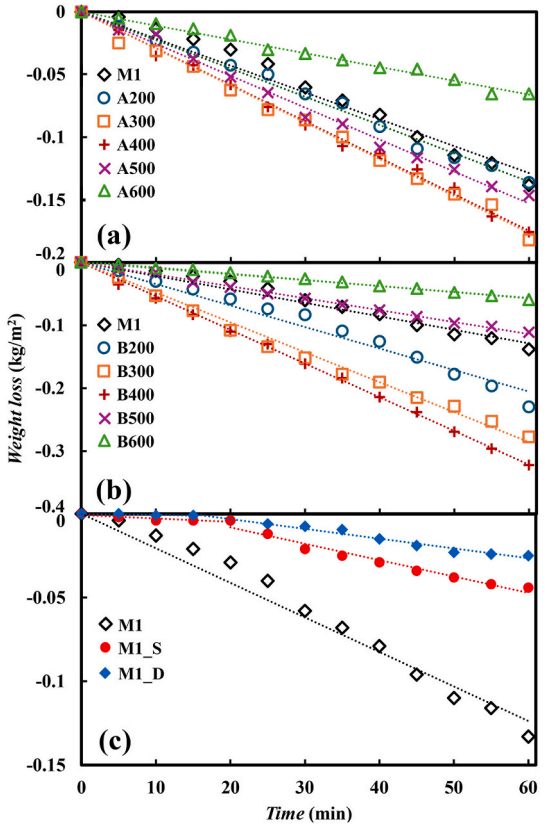

Fig. 8. Weight loss during the erosion cycles of A samples (treated for 10 min) (a), B samples (treated for 60 min) (b), and M1 samples treated with bio-based polymers (c).

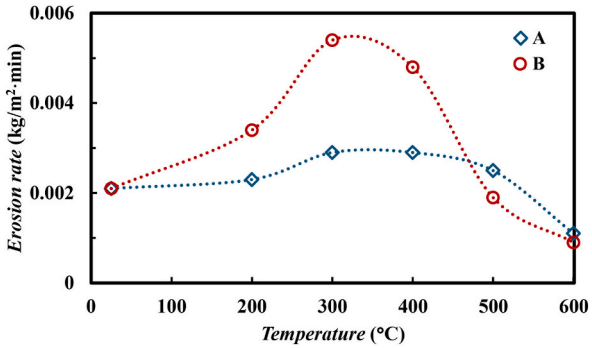

Fig. 9. ER of heat-treated samples at different temperatures: 10 min (⋄) and 60 min (○).

This phenomenon can be attributed to the fact that, up to 400 °C, dehydration weakens the cohesion of the matrix, making the material more fragile and susceptible to impacts. This effect is more pronounced in samples treated for 60 min, as deeper dehydration involves the water in the innermost parts of the samples. This behaviour is further supported by the weight loss observed in the thermally treated samples (Table 4), which highlights higher weight loss percentages in the samples treated for 60 min.

At temperatures above 400 °C, the dehydration process is accompanied by dihydroxylation [79]. This phenomenon is also observed in the samples treated at 500 °C for 10 min, which, however, show only a slight improvement compared to the samples treated at 400 °C, 300 °C, and 200 °C, due to the short duration of the treatment, without surpassing the performance of untreated samples. In these cases, the dehydroxylation processes are less developed, explaining the lower resistance compared to samples subjected to a 60-min treatment at the same temperature.

Furthermore, from Fig. 9, it can be observed that the ER of the samples treated at temperatures below 400 °C show significant differences between the two treatment durations. However, starting from 500 °C, the values become closer and show a high degree of

similarity, particularly at 600 °C, where they reach $1.1{\cdot}10^{-3}$ kg $m^{-2}{\cdot}min^{-1}$ and $0.9{\cdot}10^{-3}$ kg $m^{-2}{\cdot}min^{-1}$ for treatment durations of 10 and 60 min, respectively. This is further confirmed by the similarity of the XRD patterns at 600 °C for the 10 and 60 min treatments, where no evidence of the low-angle peaks associated with clay minerals is observed.

The temperature and duration of the heat treatment significantly influence erosion resistance. Longer treatment times amplify both the negative effects of dehydration (at temperatures below 400 °C) and the positive effects of dehydroxylation (at temperatures above 500 °C). Specifically, at 600 °C, the treatment duration becomes less influential, as the sets of samples treated at this temperature exhibit similar ER.

Samples treated with bio-based polymers exhibit significant resistance to erosion, particularly during the first four cycles (Fig. 8 c). However, after this initial phase, microcracks begin to form, especially in areas where the penetration of polymer is more difficult for surface irregularity. These microcracks progressively lead to more intense and localized erosion as the cycles continue, resulting in a change in the slope of the erosion trend and a corresponding increase in the ER. Specifically, the ER increases from $0.08{\cdot}10^{-3}$ kg $m^{-2}{\cdot}min^{-1}$ to $0.6{\cdot}10^{-3}$ kg $m^{-2}{\cdot}min^{-1}$ for polymer S after the third cycle and from $0.2{\cdot}10^{-3}$ kg $m^{-2}{\cdot}min^{-1}$ to $1{\cdot}10^{-3}$ kg $m^{-2}{\cdot}min^{-1}$ for polymer D after the fourth cycle, reaching values comparable to those of samples thermally treated at 600 °C. In areas where the polymer film is damaged, the surface degrades similarly to untreated samples, with the exposed area increasing with each cycle, as visually shown in Fig. 10k and l. While the polymer coating is effective at protecting the surface from erosion initially, even a single weak point can significantly accelerate the erosion process, ultimately compromising the protective effect due to the limited penetration depth of this treatment. By comparing Fig. 10a–j with Fig. 6a–j, it is evident that thermal treatment provides uniform protection, even in the subsurface layers. The colour, indicative of dehydration and dehydroxylation processes, does not change beneath the eroded surface, suggesting good penetration of the treatment. This effect can be estimated to reach at least 3 mm in depth, considering the 6 mm thickness of the sample exposed on both sides to the treatment temperatures.

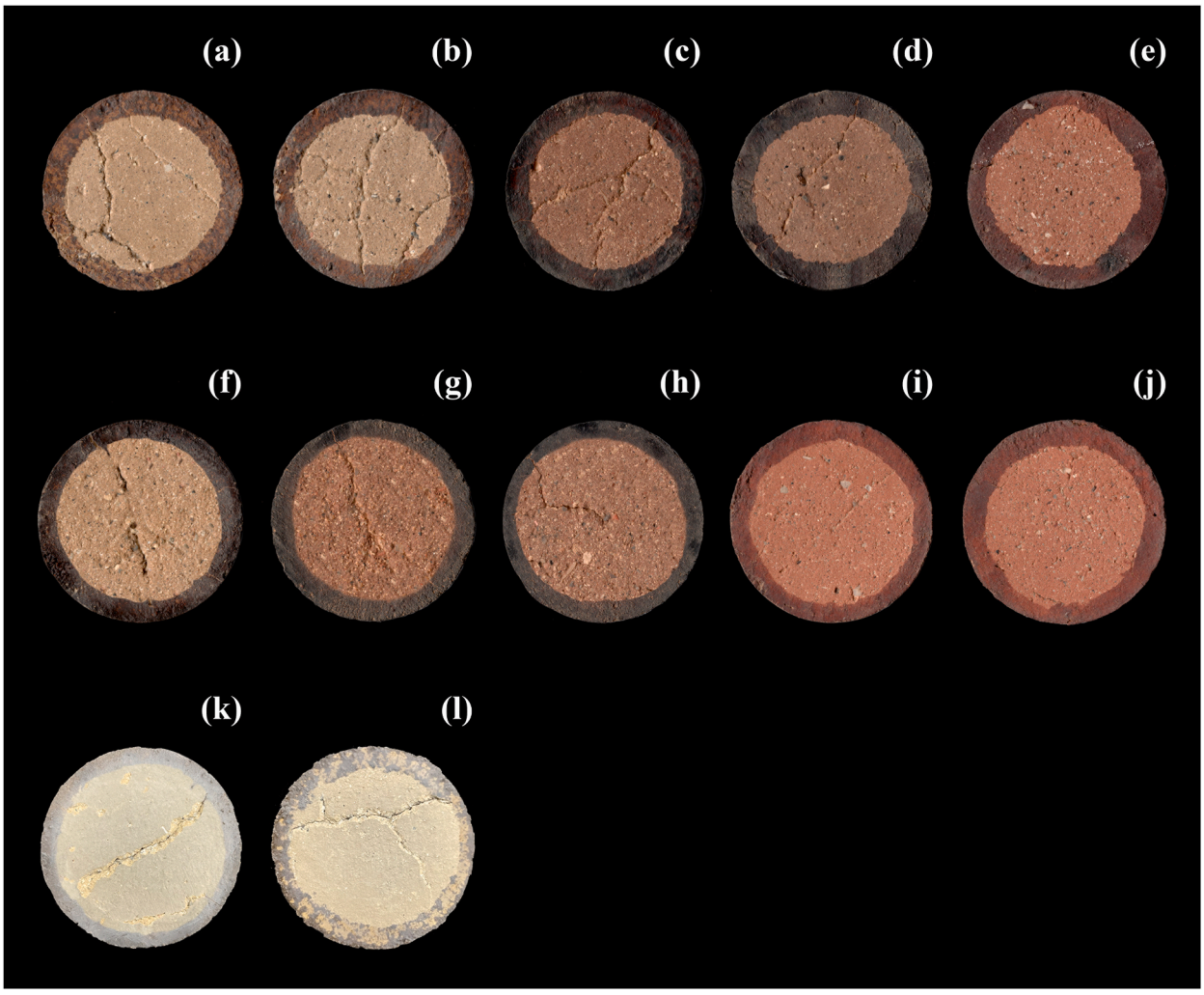

Fig. 10. Surfaces of the samples subjected to superficial stabilization after the erosion cycles: A200 (a); A300 (b); A400 (c); A500 (d); A600 (e); B200 (f); B300 (g); B400 (h); B500_60 (i); B600 (j); M1_S (k); M1_D (l).

3.5. Water resistance and wet-dry cycles on M1 treated samples

Regarding water resistance, the C1_442 samples, surface-stabilized, were subjected to a total imbibition test for a duration of 360 min at room temperature. The results for water resistance time (WRT) and the volume of voids accessible to water (P_{H2O}) are presented in Table 5.

In untreated samples, the loss of cohesion occurred immediately, leading to the complete disintegration of the samples within the first minute of immersion. In contrast, samples A200, A300, B200, and B300 exhibited slightly longer cohesion times, resisting for 3, 5, 6, and 15 min, respectively. However, the disintegration mechanism was similar to that of untreated samples, with grain detachment caused by the loss of cohesion between particles. This made it impossible to measure the final weight of the sample to determine the porosity accessible to water.

A different behaviour was observed in samples A400, which resisted imbibition for 20 min. These samples fractured due to the development of cracks and fissures, eventually undergoing fragmentation into multiple parts. Another observation for this series (A400) was a degree of plasticity detected in the material when the first cracks appeared. Similarly, samples B400 showed comparable behaviour but with significantly higher imbibition times, resisting for 220 min.

The increased resistance times during total immersion suggest that even at low temperatures and short durations, thermal treatments induce slight but measurable changes in grain cohesion and resistance to disintegration caused by prolonged exposure to water. For samples treated at 500 °C and 600 °C, both for 10 and 60 min, no cracking or grain decohesion was observed during the 6-h imbibition test, indicating significantly higher stability compared to treatments at lower temperatures.

The water-accessible porosity (P_{H2O}) was evaluated for samples treated at 400 °C, 500 °C, and 600 °C. The results, presented in Table 5, show that porosity remained largely unchanged across these temperatures and treatment durations by varying between about 21 and 24 %. This behaviour suggests that within this temperature range and treatment durations, microstructural transformations are still in their early stages and not advanced enough to produce substantial changes in the material's porous structure. Thermal treatments are known to induce contraction of the clay lattice; however, at these temperatures and durations, such contraction is minimal and insufficient to cause significant modifications to water-accessible porosity. The consistent P_{H2O} values therefore indicate a relative stability of the porous structure within this temperature range and treatment conditions. In conclusion, the stability of water-accessible porosity in samples treated at 400 °C, 500 °C, and 600 °C reflects the limited extent of heat-induced microstructural changes under these conditions. To observe significant variations in porosity, higher temperatures or longer treatment durations would be required.

The samples treated with bio-based polymers S and D exhibited similar behaviour in terms of breaking and disintegration modes, but with a significant difference in water stability. Specifically, the samples treated with bio-based polymer S demonstrated nearly double the water resistance compared to those treated with bio-based polymer D, with resistance times of 140 min and 80 min, respectively. As observed in the case of erosion, the areas where the polymer film showed less penetration acted as weak points. In these locations, water was able to penetrate the sample, leading to progressive saturation through a slow absorption process. During the initial stages of imbibition, stains were observed at various points on the surface, indicating the low penetration of the polymer film coating in some points (Fig. 11 a and d).

In the stages preceding the disintegration of the sample, the polymer film enveloped the grains like a wrapping (Fig. 11 c), causing the material to lose its structural integrity. However, as the process continued, the film began to disintegrate at the edges. This led to the progressive detachment of the surface film (Fig. 11 f) and ultimately to the complete disintegration of the sample.

This behaviour highlights the importance of the continuity and integrity of the polymer film in protecting materials. The difficulty in ensuring a uniform application of the bio-based polymer, particularly in the presence of protruding grains, presents a significant challenge in enhancing the effectiveness of the treatment, both in terms of erosion resistance and water stability.

The wet-dry cycles have confirmed the findings observed during total water imbibition tests. Samples heat treated at 200 °C and 300 °C, for both tested durations, failed to complete the first 20-min imbibition cycle, disintegrating within the previously reported timeframes. Samples A400 exhibited minor cracks and slight plasticity at the end of the first imbibition cycle. Subsequent heating at 160 °C caused 80 % of the tested samples to fragment into multiple pieces upon re-immersion in water at the start of the second cycle. In contrast, samples from the B400 series successfully completed an average of 4 ± 1 cycles before fracturing. Samples from the A500 series, despite completing the 6-h total imbibition test, failed to withstand the wet-dry cycles, breaking after 11 ± 2 cycles. Meanwhile, samples B500, A600, and B600 successfully completed 40 cycles without any weight variation, demonstrating excellent water resistance and durability under repeated wet-dry conditions and associated thermohygrometric stress.

The series of samples treated with bio-based polymers completed 1 cycle (M1_S) and 4 cycles (M1_D), respectively. In both cases, surface staining was observed during the first imbibition cycle, indicating that in some areas the polymer coating lost continuity due to slight surface roughness. These stains increased in number following oven heating at 160 °C, attributed to the decomposition of the polymer. The samples subsequently lost their structural integrity, ultimately fracturing due to peeling of the coating.

4. Conclusions

In this work, a procedure was proposed for the stabilization of sustainable earth-based materials (systems M1, M2, M3) through low-temperature thermal treatments (200–600 °C) and different exposure times (10 and 60 min), in comparison with systems treated with biopolymers (S and D). Stabilization was verified in terms of surface erosion resistance and through wet–dry cycles.

Table 5
WRT and P_{H2O} of stabilized samples.

Sample	WRT (min)	P_{H2O} (%)
M1	1 ± 0.25	–
A200	3 ± 0.12	–
A300	5 ± 1.2	–
A400	20 ± 1.2	22.83
A500	360	22.02
A600	360	22.76
B200	6 ± 1	–
B300	15 ± 2.6	–
B400	220 ± 6.3	23.54
B500	360	21.83
B600	360	23.79
M1_S	140 ± 4.3	–
M1_D	80 ± 6.1	–

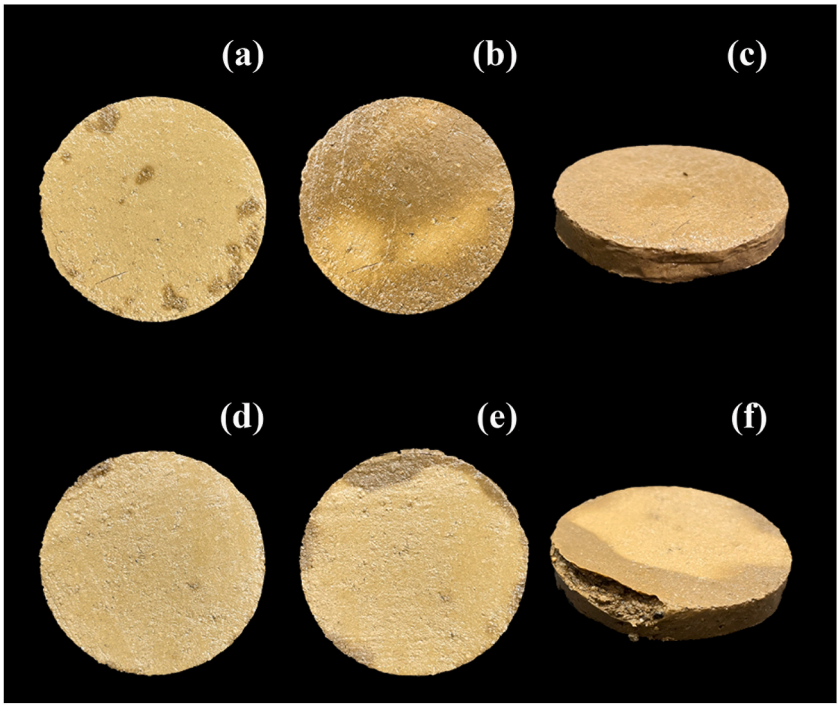

Fig. 11. Sample M1_S after 1 min (a), 18 min (b) and 135 min (c) of absorption test; Sample M1_D after 1 min (a), 11 min (b) and 80 min (c) of absorption test.

1. Erosion resistance. For the evaluation of the erosion rate, an original technique was used based on the Spex Mixer/Mill, which is widely employed in other fields such as mechanochemistry for powder grinding and the mechanical activation of chemical reactions. The jar, containing an erodent, was set in motion by the mill's mechanism and modified so that one of its closing surfaces was replaced with the sample to be tested. The test lasted 5 min and was cyclically repeated 12 times, measuring the weight loss at each step. At the end of the erosion tests, mixture M1, with a higher clay content, showed superior erosion resistance due to plastic deformation of the matrix and a smoother surface structure and was thus selected for stabilization.
2. Effects of thermal treatments. Up to 400 °C, partial dehydration weakens cohesion, increasing erosion susceptibility, particularly in systems treated for 60 min. At 500–600 °C, clay dehydroxylation leads to an improvement in erosion rate and water stability. In particular, samples treated at 600 °C for both exposure times reached erosion rate values of approximately $1{\cdot}10^{-3}$ kg $m^{-2}{\cdot}min^{-1}$, lower than those of untreated samples and those treated at lower temperatures, and successfully completed 40 wet–dry cycles without weight variations, demonstrating the potential for shorter processing times at higher temperatures. Water resistance under total absorption conditions varied depending on the thermal treatment temperature and duration.
3. Performance of bio-based polymers. Treatments with the biopolymers used to obtain systems S and D provided excellent initial protection against erosion (low ER) but led to the formation of microcracks and subsequent localized degradation which, after about the fourth cycle, resulted in erosion rate values comparable to those of systems treated at the highest temperatures.

Resistance to wet–dry cycles was considerably lower (S: 1 cycle; D: 4 cycles). Water resistance in terms of total absorption was significantly improved, but the continuity of the polymer film proved essential for ensuring the durability of the sample.

These results highlight how low-temperature thermal treatments with short exposure times represent a potential alternative to conventional binders (lime, cement) in specific applications (small-scale buildings, architectural elements with moderate durability, etc.), allowing for the development of materials with adequate mechanical and hygrometric performance without the need to introduce non-recyclable organic components. The use of recycled aggregates from previous demolitions promotes sustainability by reducing embodied emissions and the environmental impact associated with quarrying raw materials.

In the future, it will be necessary to quantify the overall footprint of the selected treatments through a life cycle assessment (LCA), with reference to the benefits in terms of strength, durability, and reversibility of the intervention.

CRediT authorship contribution statement

Marta Cappai: Writing – review & editing, Writing – original draft, Visualization, Validation, Methodology, Investigation, Formal analysis, Data curation, Conceptualization. **Giorgio Pia:** Writing – review & editing, Writing – original draft, Visualization, Validation, Supervision, Resources, Project administration, Methodology, Investigation, Funding acquisition, Conceptualization.

Funding sources

This research did not receive any specific grant from funding agencies in the public, commercial, or not-for-profit sectors.

Declaration of competing interest

The authors declare that they have no known competing financial interests or personal relationships that could have appeared to influence the work reported in this paper.

Acknowledgements

The authors are grateful to R.E.R. s.r.l. and Matteo Brioni s.r.l. for providing the raw materials necessary for this work. Special thanks are also extended to Dr. Justin Byron Blanco and Dr. Antonio Porcu for their support during the laboratory activities.

Data availability

Data will be made available on request.

References

[1] B. Sizirici, Y. Fseha, C.S. Cho, I. Yildiz, Y.J. Byon, A review of carbon footprint reduction in construction industry, from design to operation, Materials 14 (2021), https://doi.org/10.3390/ma14206094.
[2] Y.H. Labaran, V.S. Mathur, S.U. Muhammad, A.A. Musa, Carbon footprint management: a review of construction industry, Clean Eng. Technol. 9 (2022), https://doi.org/10.1016/j.clet.2022.100531.
[3] Z. Huang, H. Zhou, Z. Miao, H. Tang, B. Lin, W. Zhuang, Life-cycle carbon emissions (LCCE) of buildings: implications, calculations, and reductions, Engineering 35 (2024) 115–139, https://doi.org/10.1016/j.eng.2023.08.019.
[4] Á. Lakatos, Novel thermal insulation materials for buildings, Energies 15 (2022), https://doi.org/10.3390/en15186713.
[5] F. Mneimneh, H. Ghazzawi, S. Ramakrishna, Review study of energy efficiency measures in favor of reducing carbon footprint of electricity and power, buildings, and transportation, Circ. Econ. Sustain. 3 (2023) 447–474, https://doi.org/10.1007/s43615-022-00179-5.
[6] M. Abdellatief, L.S. Wong, N.M. Din, A.N. Ahmed, A.M. Hassan, Z. Ibrahim, G. Murali, K.H. Mo, A. El-Shafie, Sustainable foam glass property prediction using machine learning: a comprehensive comparison of predictive methods and techniques, Results Eng. 25 (2025), https://doi.org/10.1016/j.rineng.2025.104089.
[7] W. Villasmil, L.J. Fischer, J. Worlitschek, A review and evaluation of thermal insulation materials and methods for thermal energy storage systems, Renew. Sustain. Energy Rev. 103 (2019) 71–84, https://doi.org/10.1016/j.rser.2018.12.040.
[8] European Commission, Stepping up Europe's 2030 climate ambition. Investing in a climate-neutral future for the benefit of our people. https://eur-lex.europa.eu/legal-content/EN/TXT/PDF/?uri=CELEX:52020DC0562, 2020. (Accessed 7 January 2025).
[9] United Nations Environment Programme, Building Materials and the Climate: Constructing a New Future, 2023.
[10] H.A. Vaghefi-Rezaee, H. Sarvari, S. Khademi-Adel, D.J. Edwards, C.J. Roberts, A scientometric review and analysis of studies on the barriers and challenges of sustainable construction, Buildings 14 (2024), https://doi.org/10.3390/buildings14113432.
[11] United Nations Environment Programme, Global Status Report for Buildings and Construction. Beyond foundations: mainstreaming sustainable solutions to cut emissions from the buildings sector. https://doi.org/10.59117/20.500.11822/45095, 2024.
[12] United Nations Environment Programme, 2022 global status report for buildings and construction: towards a zero-emission, efficient and resilient buildings and construction sector. www.globalabc.org, 2022.
[13] F. Pacheco-Torgal, S. Jalali, Earth construction: lessons from the past for future eco-efficient construction, Constr. Build. Mater. 29 (2012) 512–519, https://doi.org/10.1016/j.conbuildmat.2011.10.054.
[14] F.P. Torgal, S. Jalali, Eco-efficient Construction and Building Materials, Springer-Verlag London, 2011, https://doi.org/10.1017/CBO9781107415324.004.
[15] H. Schroeder, Sustainable building with earth. https://doi.org/10.1007/978-3-319-19491-2, 2015.
[16] A. Fabbri, J.C. Morel, Earthen materials and constructions, in: Nonconventional and Vernacular Construction Materials, Elsevier, 2016, pp. 273–299, https://doi.org/10.1016/B978-0-08-100038-0.00010-X.
[17] UNESCO, Earthen architecture in today's world, in: E. Lazare, J. Thierry (Eds.), Proceedings of the UNESCO International Colloquium on the Conservation of World Heritage Earthen Architecture, Architecture, 17-18 December 2012, United Nations Educational, Scientific and Cultural Organization, 2013. http://whc.unesco.org/en/series/.

[18] H. Hugo, H. Guillard, Earth Construction: A Comprehensive Guide, 1994.
[19] L. Ben-Alon, A.R. Rempel, Thermal comfort and passive survivability in earthen buildings, Build. Environ. 238 (2023) 110339, https://doi.org/10.1016/j.buildenv.2023.110339.
[20] M.R. Hall, S. Casey, Hygrothermal behaviour and occupant comfort in modern earth buildings, Modern Earth Buildings: materials, Eng. Constr. Appl. (2012) 17–40, https://doi.org/10.1533/9780857096166.1.17.
[21] I. Costa-Carrapiço, J.N. González, R. Raslan, C. Sánchez-Guevara, M.D.R. Marrero, Understanding thermal comfort in vernacular dwellings in Alentejo, Portugal: a mixed-methods adaptive comfort approach, Build. Environ. 217 (2022), https://doi.org/10.1016/j.buildenv.2022.109084.
[22] L. Casnedi, M. Cappai, A. Cincotti, F. Delogu, G. Pia, Porosity effects on water vapour permeability in earthen materials: experimental evidence and modelling description, J. Build. Eng. 27 (2020), https://doi.org/10.1016/j.jobe.2019.100987.
[23] A.T.M. Marsh, Y. Kulshreshtha, The state of earthen housing worldwide: how development affects attitudes and adoption, Build. Res. Inf. 50 (2022) 485–501, https://doi.org/10.1080/09613218.2021.1953369.
[24] H. Van Damme, H. Houben, Earth concrete. Stabilization revisited, Cement Concr. Res. 114 (2016) 90–102, https://doi.org/10.1016/j.cemconres.2017.02.035.
[25] P. Walker, R. Keable, J. Martin, V. Maniatidis, Rammed Earth: Design and Construction Guidelines, PublisherIHS BRE, 2005.
[26] D. Rocha, P. Faria, S.S. Lucas, Additive manufacturing of earth-based materials: a literature review on mortar composition, extrusion, and processing earth, Materials 17 (2024) 1–27, https://doi.org/10.3390/ma17010202.
[27] T. Santos, L. Nunes, P. Faria, Production of eco-efficient earth-based plasters: influence of composition on physical performance and bio-susceptibility, J. Clean. Prod. 167 (2017) 55–67, https://doi.org/10.1016/j.jclepro.2017.08.131.
[28] L. Miccoli, U. M??ller, P. Fontana, Mechanical behaviour of earthen materials: a comparison between earth block masonry, rammed earth and cob, Constr. Build. Mater. 61 (2014) 327–339, https://doi.org/10.1016/j.conbuildmat.2014.03.009.
[29] M. Gernot, Building with earth, thirdand r. https://doi.org/10.3362/9781780443959, 2013.
[30] R. Rael, Earth Architecture, Princeton, 2009.
[31] G.J. Frencham, The Performance of Earth Buildings, 1982.
[32] P. De Joanna, The earthen architecture and standards requirements, Smc 1 (2014) 70–74.
[33] A.M. de F. Luiz, S.A.L. Bessa, M.A.P. Rezende, Trends and innovations in earthen plaster mix design: a review, J. Build. Eng. 98 (2024), https://doi.org/10.1016/j.jobe.2024.111346.
[34] Y. Zhang, J. Liu, J. Yue, H. Su, Experimental study on improving the performance of imitation earthen site soil in carbon dioxide environment, J. Build. Eng. 95 (2024), https://doi.org/10.1016/j.jobe.2024.110338.
[35] T. Santos, N.W. Luijten, A. Santos Silva, J.D. Silvestre, P. Faria, Earthen plasters hygrothermal and mechanical performance: effect of adding recycled gypsum from plasterboards and raw hemihydrate, J. Build. Eng. 98 (2024), https://doi.org/10.1016/j.jobe.2024.111407.
[36] K.A. Heathcote, Durability of earthwall buildings, Constr. Build. Mater. 9 (1995) 185–189, https://doi.org/10.1016/0950-0618(95)00035-E.
[37] E. Quagliarini, M. D'Orazio, S. Lenci, The Properties and Durability of Adobe Earth-Based Masonry Blocks, Elsevier Ltd, 2014, https://doi.org/10.1016/B978-1-78242-305-8.00016-4.
[38] C.T.S. Beckett, P.A. Jaquin, J.C. Morel, Weathering the storm: a framework to assess the resistance of earthen structures to water damage, Constr. Build. Mater. 242 (2020) 118098, https://doi.org/10.1016/j.conbuildmat.2020.118098.
[39] M. Cappai, F. Delogu, D. Pozzi-Escot, G.P. Neyra, P. Meloni, G. Pia, Degradation phenomena of Templo Pintado painted plasters, Constr. Build. Mater. 392 (2023) 131839, https://doi.org/10.1016/j.conbuildmat.2023.131839.
[40] M. Cappai, L. Casnedi, G. Carcangiu, F. Delogu, D. Pozzi-escot, G. Pacheco, G. Pia, P. Meloni, Weathering of earth-painted surfaces : environmental monitoring and artificial aging, Constr. Build. Mater. 344 (2022) 128193, https://doi.org/10.1016/j.conbuildmat.2022.128193.
[41] P. Faria, T. Santos, J.E. Aubert, Experimental characterization of an earth eco-efficient plastering mortar, J. Mater. Civ. Eng. 28 (2016), https://doi.org/10.1061/(ASCE)MT.1943-5533.0001363.
[42] J. Lima, P. Faria, Eco-efficient Earthen Plasters: the Influence of the Addition of Natural Fibers, vol. 12, RILEM Bookseries, 2016, pp. 315–327, https://doi.org/10.1007/978-94-017-7515-1_24.
[43] S. Liuzzi, C. Rubino, F. Martellotta, Properties of Clay Plasters with Olive Fibers, LTD, 2020, https://doi.org/10.1016/b978-0-12-819481-2.00009-x.
[44] A. Thomson, D. Maskell, P. Walker, M. Lemke, A. Shea, M. Lawrence, Improving the hygrothermal properties of clay plasters. 15th International Conference on Non-conventional Materials and Technologies (NOCMAT 2015), 2015, p. 8.
[45] T. Ashour, H. Wieland, H. Georg, F.J. Bockisch, W. Wu, The influence of natural reinforcement fibres on insulation values of earth plaster for straw bale buildings, Mater. Des. 31 (2010) 4676–4685, https://doi.org/10.1016/j.matdes.2010.05.026.
[46] J.L. Parracha, A.S. Pereira, R.V. da Silva, V. Silva, P. Faria, Effect of innovative bioproducts on the performance of bioformulated earthen plasters, Constr. Build. Mater. 277 (2021) 122261, https://doi.org/10.1016/j.conbuildmat.2021.122261.
[47] N. Sohaib, M.S. Faiz, G. Sana, Use of Acrylic polymer for stabilization of clayey soil, Int. J. Sci. Eng. Res. 9 (2018) 433–438.
[48] A.E. Losini, A.C. Grillet, M. Bellotto, M. Woloszyn, G. Dotelli, Natural additives and biopolymers for raw earth construction stabilization – a review, Constr. Build. Mater. 304 (2021) 124507, https://doi.org/10.1016/j.conbuildmat.2021.124507.
[49] M.I. Gomes, P. Faria, T.D. Gonçalves, Earth-based mortars for repair and protection of rammed earth walls. Stabilization with mineral binders and fibers, J. Clean. Prod. 172 (2018) 2401–2414, https://doi.org/10.1016/j.jclepro.2017.11.170.
[50] A.S. Rieppi Godoy, L.E. Peisino, G. Rolón, B.B. Raggiotti, Firing the wall: a novel way to protect earth buildings, Constr. Build. Mater. 445 (2024), https://doi.org/10.1016/j.conbuildmat.2024.137878.
[51] C. Atzeni, G. Pia, U. Sanna, N. Spanu, Surface wear resistance of chemically or thermally stabilized earth-based materials, Mater. Struct. 41 (2008) 751–758, https://doi.org/10.1617/s11527-007-9278-1.
[52] C. Turco, A.C. Paula Junior, E.R. Teixeira, R. Mateus, Optimisation of Compressed Earth Blocks (CEBs) using natural origin materials: a systematic literature review, Constr. Build. Mater. 309 (2021) 125140, https://doi.org/10.1016/J.CONBUILDMAT.2021.125140.
[53] J. Nakamatsu, S. Kim, J. Ayarza, E. Ramírez, M. Elgegren, R. Aguilar, Eco-friendly modification of earthen construction with carrageenan: water durability and mechanical assessment, Constr. Build. Mater. 139 (2017) 193–202, https://doi.org/10.1016/j.conbuildmat.2017.02.062.
[54] G. Alhaik, M. Ferreira, V. Dubois, E. Wirquin, S. Tilloy, E. Monflier, G. Aouad, Enhance the rheological and mechanical properties of clayey materials by adding starches, Constr. Build. Mater. 139 (2017) 602–610, https://doi.org/10.1016/j.conbuildmat.2016.11.130.
[55] H. Van Damme, H. Houben, Should Raw Earth Be Improved ? An Environmental Assessment, Actes Du 12ème Congrès Mondial Sur Les Architectures de Terre - TERRA 2016, 180–182, http://www.amaco.org/spiral-files/download?mode=inline&data=4558, 2016.
[56] P.J. Walker, Strength , durability and shrinkage characteristics of cement stabilised soil blocks, Cem. Concr. Compos. 17 (1995) 301–310.
[57] P. Walker, T. Stace, Properties of some cement stabilised compressed earth blocks and mortars, Mater. Struct. 30 (1997) 545–551, https://doi.org/10.1007/bf02486398.
[58] R. Shoukat, M. Cappai, G. Pia, L. Pilia, An updated review: opuntia ficus indica (OFI) chemistry and its diverse applications, Appl. Sci. 13 (2023) 7724, https://doi.org/10.3390/app13137724.
[59] R. Shoukat, M. Cappai, L. Pilia, G. Pia, Rice starch chemistry, functional properties, and industrial applications: a review, Polymers 17 (2025) 110, https://doi.org/10.3390/polym17010110.
[60] B. Ilman, A.P. Balkis, Sustainable biopolymer stabilized earthen: utilization of chitosan biopolymer on mechanical, durability, and microstructural properties, J. Build. Eng. 76 (2023), https://doi.org/10.1016/j.jobe.2023.107220.
[61] K.K.G.K.D. Kariyawasam, C. Jayasinghe, Cement stabilized rammed earth as a sustainable construction material, Constr. Build. Mater. 105 (2016) 519–527, https://doi.org/10.1016/j.conbuildmat.2015.12.189.

[62] A.W. Bruno, L.M. Lalicata, R. Abdallah, A. Lagazzo, S. Arris-Roucan, F. McGregor, C. Perlot, D. Gallipoli, Synergic effect of hydrated lime and guar gum stabilisation on the mechanical, thermal and hygroscopic behaviour of a Ligurian earth material, Constr. Build. Mater. 439 (2024), https://doi.org/10.1016/j.conbuildmat.2024.137258.
[63] S. Real, J.A. Bogas, R. Cruz, M.G. Gomes, Eco-recycled cement's effect on the microstructure and hygroscopic behaviour of compressed stabilised earth blocks, J. Build. Eng. 95 (2024), https://doi.org/10.1016/j.jobe.2024.110227.
[64] E. Levačić, B. Mladen, Soil stabilization by means of "LENDUR EH" ureaformaldehyde resin, Mining-Geol.-Pet. Eng. Bull. 2 (1990) 137–143.
[65] S.N. Malkanthi, N. Balthazaar, A.A.D.A.J. Perera, Lime stabilization for compressed stabilized earth blocks with reduced clay and silt, Case Stud. Constr. Mater. 12 (2020), https://doi.org/10.1016/j.cscm.2019.e00326.
[66] C. Atzeni, F. Bodano, U. Sanna, N. Spanu, Surface strength: definition and testing by a sand impact method, J. Cult. Herit. 7 (2006) 201–205, https://doi.org/10.1016/j.culher.2006.05.002.
[67] R. Striani, M. Cappai, L. Casnedi, C.E. Corcione, G. Pia, Coating's influence on wind erosion of porous stones used in the Cultural Heritage of Southern Italy: surface characterisation and resistance, Case Stud. Constr. Mater. 17 (2022) e01501, https://doi.org/10.1016/j.cscm.2022.e01501.
[68] D. Camuffo, Controlling the aeolian erosion of the great sphinx, Stud. Conserv. 38 (1993) 198–205, https://doi.org/10.2307/1506380.
[69] Y. Hao, Y. Feng, J. Fan, Experimental study into erosion damage mechanism of concrete materials in a wind-blown sand environment, Constr. Build. Mater. 111 (2016) 662–670, https://doi.org/10.1016/j.conbuildmat.2016.02.137.
[70] X. Cai, Z. He, S. Tang, X. Chen, Abrasion erosion characteristics of concrete made with moderate heat Portland cement, fly ash and silica fume using sandblasting test, Constr. Build. Mater. 127 (2016) 804–814, https://doi.org/10.1016/j.conbuildmat.2016.09.117.
[71] A. Noreen, K.M. Zia, M. Zuber, S. Tabasum, A.F. Zahoor, Bio-based polyurethane: an efficient and environment friendly coating systems: a review, Prog. Org. Coat. 91 (2016) 25–32, https://doi.org/10.1016/j.porgcoat.2015.11.018.
[72] M. Cappai, R. Shoukat, L. Pilia, R. Ricciu, D. Lai, G. Marongiu, G. Pia, Thermal properties of eco-friendly earthen materials stabilized with bio-based polymers: experimental data and modeling procedure for improving mix-design, Materials 17 (2024) 1035, https://doi.org/10.3390/ma17051035.
[73] N. Karak, Biopolymers for paints and surface coatings. https://doi.org/10.1016/B978-0-08-100214-8.00015-4, 2016.
[74] C. Dizman, E.C. Kaçakgıl, Alkyd resins produced from bio-based resources for more sustainable and environmentally friendly coating applications, Turk. J. Chem. 47 (2023) 1–23, https://doi.org/10.55730/1300-0527.3511.
[75] C. Suryanarayana, Mechanical alloying and milling, Prog. Mater. Sci. 46 (2001) 1–184, https://doi.org/10.1016/S0079-6425(99)00010-9.
[76] D. Camuffo, Physical weathering of stones, Sci. Total Environ. 167 (1995) 1–14, https://doi.org/10.1016/0048-9697(95)04565-I.
[77] M.C. Gastuche, F. Toussaint, J.J. Fripiat, R. Touilleaux, M. Van Meersche, Study of intermediate stages in the kaolin→ metakaolin transformation, Clay Miner. Bull. 29 (1963) 227–236.
[78] Y.O. Abiodun, O.M. Sadiq, S.O. Adeosun, G.L. Oyekan, Mineralogical properties of kaolin and metakaolin from selected areas in Nigeria and its application to concrete production, West Indian J. Eng. 1 (2019).
[79] L. Heller-Kallai, Chapter 7.2 thermally modified clay minerals, in: Dev Clay Sci, 2006, pp. 289–308, https://doi.org/10.1016/S1572-4352(05)01009-3.